Journal of the Korean Chemical Society
2011, *Vol. 55, No. 4*
Printed in the Republic of Korea
DOI 10.5012/jkcs.2011.55.4.563

속 보

아연필름의 수용액내 직접산화를 통한 산화아연 나노막대 전극의 제조

박지혜 · 신유주*
가톨릭대학교 화학전공
(접수 2011. 6. 21; 수정 2011. 6. 30; 게재확정 2011. 6. 30)

Fabricaction of ZnO Nanorod Array Electrode Via Direct Oxidation of Zn Metal Film in Aqueous Solution

Ji-Hye Park and Yu-Ju Shin*
Department of Chemistry, The Catholic University of Korea, Bucheon, Gyeonggi 422-743, Korea
(Received June 21, 2011; Revised June 30, 2011; Accepted June 30, 2011)

주제어: 산화아연 나노막대전극, DSC, 스퍼터링, 수용액상 산화
Keywords: Analcime, Zeolite, Structure, Single-crystal, Si/Al ratio

One-dimensional nanorod array electrodes of ZnO have been extensively studied for various electronic device applications including electroluminescence and dye-sensitized solar cell.[1-3] Studies on the growth of ZnO-nanorod array have been carried out along two directions, gas-phase growing based on vacuum technology[4] and wet solution route using seed-growing method.[5,6] The latter has been regarded economically more adequate for large-area production with low energy consumption, especially for the application of dye-sensitized solar cells (DSC). Due to the high crystallinity of individual ZnO nanorods which enables the enhancement of the charge transport properties of injected electrons into ZnO matrix from the photo-excited sensitizer molecules, ZnO nanorod array electrode has shown the energy conversion efficiency as high as 1.5%[3], despite the small surface only capable of up-taking 10-20% of dye molecules with respect to the conventional nanoparticulate electrode. The growth of ZnO nanorod array via hydrothermal route consists of two steps, the formation of the seed layer and the growing of aligned ZnO nanorods from the seed layer.[5] Here we present an alternative to this conventional approach in which metallic Zn film is slowly converted into ZnO nanorods in aqueous solution. For this purpose, a slow oxidation of Zn metal film was induced through the formation of Zn-formamide complex at elevated temperature.

ZnO films were obtained by chemical oxidation of Zn metal films on FTO glass (Pilkington Glass, TEC8) in 5 wt% formamide aqueous solution.[7] Zn metal was firstly deposited using DC magnetron sputtering equipment (Cressington 108) with 2-inch Zn target (Sigma Aldrich 99.9%) placed at 2 cm above the substrate. The current was controlled to be 25 mA under 100 mtorr of Ar. The sputtering time was controlled for 1 min (Z1) and 5 min (Z2), respectively. The deposition area was fixed 1×1 cm^2 to ensure homogenous deposition. The Zn metal films were put into 5 wt% formamide aqueous solution (300 mL) and oxidized at 65 °C for 40 h, resulting in ZO1 and ZO2 respectively. Zn metal was deposited once again on ZO1 film for 5 min under the same sputtering condition, followed by the oxidation in formamide solution, leading to the ZnO nanorod array electrode (ZR). To remove eventual trace of Zn metal component, the ZnO nanorod electrode was heated at 400 °C under O_2 flow for 15min before sensitizing them for DSSC. The ZO2 and ZR electrodes were sensitized with 0.30 mM ethanolic solution of ruthenium dye Ru[dcbpy(TBA)$_2$]$_2$(NCS)$_2$ (known as N719) for 2 h at 60 °C. Dye-sensitized ZnO electrode and Pt-coated counter electrode were assembled with 30-ìm thick Surlyn (Dupont) as a spacer. The redox electrolyte solution consisted of 0.6 M 1-hexyl-2,3-dimethyl imidazolium iodide (C6DMI), 0.2M LiI, 0.04M I_2 and 0.5M *tert*-butyl pyridine (TBP) in 3-methoxy propionitrile (MPN)/acetonitrile (ACN) (1:1 v/v).

Scanning electron microscopy (SEM) was carried out using Hitachi S-4800. X-ray diffraction patterns were obtained with Siemens D5005 diffractometer equipped with a curved graphite single crystal as a monochromator.

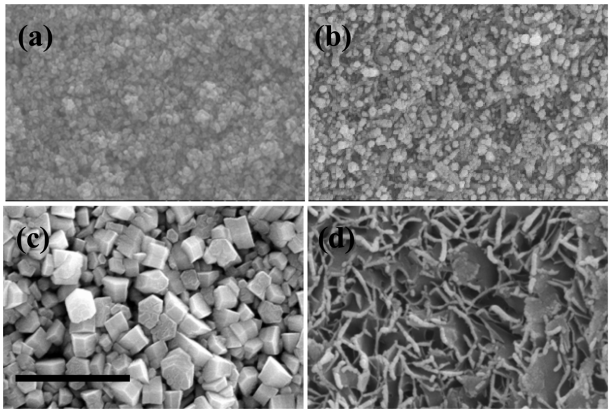

***Fig.* 1.** FE-SEM pictures of Z1 (a), ZO1(b), Z2(c) and ZO2(d). Scale bar is of 1 μm.

Photovoltaic J-V measurement of DSSC using ZnO nanorod electrode was obtained under AM1.5 global condition satisfied with a solar simulator (Yamashida Denco, Class A). The light was homogeneous for the area 5 × 5 cm^2 and the intensity was calibrated with a standard single-crystal Si-cell confirmed by NREL.

The SEM images in *Fig.* 1 show the morphologies of Zn films Z1, Z2 and their oxidized ZO1 and ZO2 films. Zn metal grains increased from particulate shape (50 nm) to hexagonal plate (250 nm) as with the sputtering time. The oxidation of these Zn films into ZnO layers were carried out for 40 h. The ZnO films ZO1 and ZO2 showed topotatic oxidation maintaining the morphological features of the initial Zn metal films, i.e. the spread nanoparticles in *Fig.* 1(b), and sheet-like shape in (d) respectively. Without formamide, the oxidation in aqueous solution occurred slower and and ZnO particles were disintegrated from substrate and thus ZnO film could not be properly formed. It was regarded that the formamide acted like an eching agent to remove Zn atoms from the surface in this work. Actually the particle sizes of ZnO in *Fig.* 1(b) and (d) similar to the initial Zn metal particles suggest that the surface Zn metal atoms were dissolved during the oxidation, otherwise the resulting ZnO should have been much larger than observed. The failure of formation of ZnO film without formamide also supports this explanation.

In *Fig.* 2, SEM pictures and X-ray diffraction (XRD) patterns of the sputtered Zn film on ZO1 (a) and ZR film (b) are represented. In contrast to Z2 which was prepared from the same sputtering condition, the Zn film on ZO1 shows that much smaller Zn particles were stacked, being highly orientated along [001]. The XRD pattern confirmed such preferred orientation of Zn film by the large intensity ratio $I_{(002)}/I_{(101)}$. It strongly suggests that the ZnO

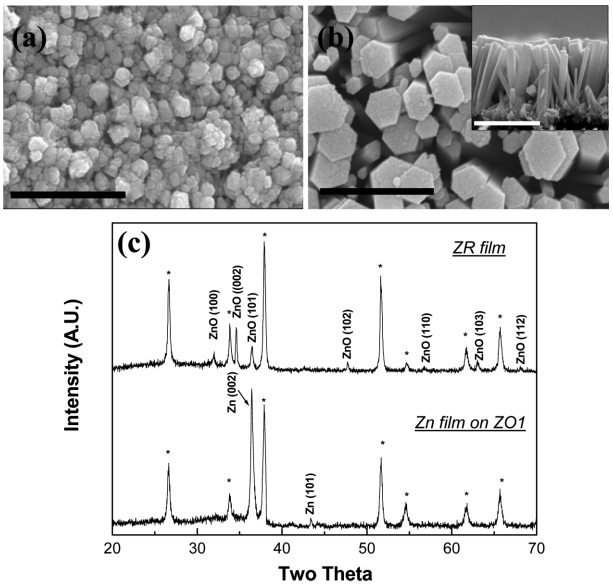

Fig. 2. FE-SEM pictures of Zn metal film sputtered on ZO1 film (a) and ZR (b). Inset shows the cross-section view. Scale bar is of 1 μm. XRD patterns of ZR film and Zn film on ZO1. *indicates substrate FTO peaks.

layer affect the crystal growth habit of Zn metal crystals dominantly oriented along [001].

A well-developed ZnO nanorod array was observed in ZR. This nanorod array also exhibited highly enhanced diffraction intensity of (002), indicating that ZnO crystals have grown with the hexagonal columnar habit along [001]. Considering the morphological differences from ZO2, the oxidation of Zn metal film should be carried out in a topotactic way to induce on-site oxidation and and thus crystallization into ZnO, avoiding complete dissolution of Zn metal into $Zn^{2+}_{(aq)}$ ions. The formation of pore channels between the nanorods may be attributed the partial removal of Zn grains through the formation of Zn-formamide complexes. The well-defined hexagonal edges of ZnO nanorods can be caused with etching by formamide, which would preferentially react with the surface Zn metal atom with high surface energy, and thus remove the surplus dangling Zn atoms located on crystal planes, finally resulting in the well-defined crystal edges. Indeed, Yu et al. reported that the oxidation of Zn metal foil by formamide induced ZnO nanotubes on Zn foil surface instead of nanorods.[7] It means that Zn metal is partially dissolved into aqueous phase as Zn^{2+} ion and the rest of Zn metal layer is oxidized into ZnO. The formation of nanorod instead of nanotube in this work may be attributed to the larger Zn particles of which boundaries were exposed to exterior. Under this circumstance, the dissolution of Zn

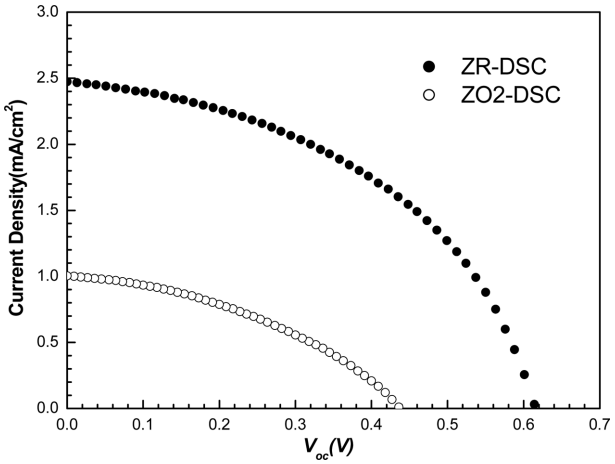

Fig. 3. J-V curves of ZR-DSC (•) and ZO2-DSC (o). ZR-DSC exhibited V_{oc}=0.616V, J_{sc}=2.474mAcm^{-2}, *ff*=46% and η=0.70%, while ZO2-DSC showed V_{oc}=0.438V, J_{sc}=1.003 mAcm^{-2}, *ff*=39.1% and η=0.17%.

metal ions by formamide should have a tendency to begin from the surface of Zn particle, leading to the hexagonal crystal planes as shown in *Fig*. 2(b). It should be also mentioned that the oxidation of Zn should result in the thickness of ZnO nanorods larger than initial Zn metal particles due to the insertion of oxygen atoms. The partial removal of Zn particles affords interspaces to which the individual ZnO nanorod expands as the oxidation proceeds. The interfused ZnO nanorods observed in *Fig*. 2(b) supports this explanation.

Fig. 3 shows the J-V curves of ZO2-DSC and ZR-DSC, respectively. Compared with ZO2-DSC, ZR-DSC showed greatly enhanced PV performance with open-circuit voltage V_{oc}=0.616V, short circuit current density J_{sc}=2.474 mAcm^{-2}, fill-factor *ff*=46% and solar energy conversion efficiency η=0.70%. Considering of the short length of ZnO nanorods around 1 μm, the photovoltaic performance is considered comparable with the previous works on ZnO nanorod-DSC.[8,9]

In summary, a simple oxidation reaction in aqueous formamide solution was found to be effective to transform Zn film into ZnO nanorod array film on FTO substrate to apply as a photoanode for DSC. More systematic investigations are now under progress to establish detailed experimental conditions to control the morphological parameters including the thickness, length and population density of ZnO nanorod array.

Acknowledgement. The authors are grateful for the financial supports from the Catholic University of Korea (grant 2009).

REFERENCES

1. Duan, X.; Huang, Y.; Cui, Y.; Wang, J.; Lieber, C. M.; *Nature* **2001**, *409*, 66.
2. Hunag, H. M.; Mao, S.; Feick, H.; Yan, H.; Wu, H.; Kind, H.; Weber, E,; Russo, R.; Yang, P. *Science* **2001**, *292*, 1897.
3. Law, M.; Greene, L. E.; Johnson, J. C.; Saykally, R.; Yang. P. *Nature Materials* **2005**, *4*, 455.
4. Shen, G.; Bando, Y.; Chen, D.; Liu, B.; Zhi, C.; Goldberg, D. *J. Phys. Chem. B* **2006**, *110*, 3973.
5. Vayssieres, L. *Adv. Mater.* **2003**, *15*(5), 464.
6. Greene, L. E.; Law, M.; Tan, D. H.; Montano, M.; Goldberger, J.; Somorjai, G.; Yang, P. *Nano. Lett.* **2005**, *5*(7), 1231.
7. Yu, H.; Zhang, Z.; Han, M.; Hao, X.; Zhu, F. *J. Amer. Chem. Soc.* **2005**, *127*, 2378.
8. Kim, K. S.; Kang, Y. S.; Lee, J. H.; Shin, Y. J.; Park, N. G.; Ryu, K. S.; Chang, S. H. *Bull. Korean Chem. Soc.* **2006**, *27*(2), 295.
9. Gao, Y.; Nagai, M. *Langmuir* **2006**, *22*, 3936.